

Indium Nanowires Synthesized at Ultra-fast Rate**

By *Seung Soo Oh, Do Hyun Kim, Myoung-Woon Moon, Ashkan Vaziri, Miyoung Kim, Euijoon Yoon, Kyu Hwan Oh* and John W. Hutchinson**

[*] Prof. K. H. Oh, S. S. Oh^[+], D. H. Kim, Prof. M. Kim, Prof. E. Yoon
Department of Materials Science and Engineering, Seoul National University
Seoul, 151-744 (Korea)
E-mail: kyuhwan@snu.ac.kr

Prof. J. W. Hutchinson, Dr. M. -W. Moon, Dr. A. Vaziri
School of Engineering and Applied Sciences, Harvard University
Cambridge, MA 02138 (USA)
E-mail: jhutchinson@fas.harvard.edu

Dr. M. -W. Moon
Future Fusion Technology Laboratory, Korea Institute of Science and Technology
Seoul, 136-791 (Korea)

[+] Present address: Materials Department, University of California, Santa Barbara, CA 93106 (USA)

[**] S. S. Oh and D. H. Kim contributed equally to this work. The authors thank Korea Basic Science Institute for HVEM measurement. This work was supported in part by the Ministry of Education through the BK21 Program (KHO, MK, EY), by the ERC (Center for Materials and Processes of Self-Assembly) program of MOST /KOSEF (R11-2005-048-00000-0) (EY) and by the KOSEF grant funded by the Korea government (MOST) (No. R01-207-000-10032-0 (DHK, KHO) and R0A-2007-000-10014-0 (MK)). The work also supported in part by KIST project of a contract number 2E20200 (MWM) and in part by the School of Engineering and Applied Sciences (AV, JWH). Supporting Information is available online from Wiley InterScience or from the authors.

Keywords: In nanowire, Focused Ion Beam, Fast growth, InGaN, Maskless patterning

A challenge in the development of devices at nanometer scale, which are envisioned to impact human life in the near future,^[1] is the development of economical techniques for fabrication of their building blocks.^[2-5] Nanowires, due to their unique and exquisite characteristics,^[6-8] are ideal building blocks for functional nanoscale electronic, photonic structures^[9] and nanosurgery devices.^[10, 11] Here, we report a novel phenomenon which provides a robust technique for fabrication of single crystal indium nanowires at an ultra-fast rate. Indium nanowires have peculiar temperature-dependent electrical properties, which make them attractive for various applications.^[12] For example, the electrical resistance of

indium nanowires decreases rapidly by reaching the superconducting transition temperature, which makes them more attractive in making magnetic field generators or superconducting quantum interference devices.^[13, 14] On the other hand, post processing of indium nanowires (e.g. by oxygen or nitrogen plasma treatment) can be used to create composite nanowires made from indium compound materials on the outer surface layer of the wire. Such composite nanowires have versatile applications in electronics and optoelectronic devices, for example in building biosensors, solar cells, electrodes and even memory devices.^[15-21]

The first step in our experiments is to grow indium-rich InGaN layers of 300 nm thickness epitaxially on an GaN/sapphire substrate having thickness 330 μm . Examination of the composition of the fabricated InGaN layers using X-ray diffraction (XRD) (see Materials and Methods) indicated that the layers are ~80% indium. The second step subjects the InGaN layers to direct irradiation by Ga^+ focused ion beam (FIB). It is observed that FIB irradiation results in rapid growth of straight nanowires on the surface area of the substrate as shown schematically in Fig. 1A. The movie S1 provides an example of the appearance of nanowires as the substrate is subject to FIB with an ion current density of 400 nA/cm^2 and an accelerating voltage of 10 kV (See Supporting Information Movie S1). From the onset of irradiation, nanowires start to appear after 80s and grow at an average rate of 50 nm/s until 260s, at which point the indium source in the InGaN layer is exhausted as will be explained later. Figure 1B shows four snapshots of the growth sequence for nanowires taken at 50s time intervals at the ion current density of 200 nA/cm^2 and an accelerating voltage of 10 kV, where the synthesized nanowires have lengths as large as 30 μm and diameters in the range 50~200 nm.

To examine the material characteristics of synthesized nanowires, we performed transmission electron microscopy (TEM) and energy dispersive x-ray spectroscopy (EDS). We used these techniques to examine nanowires synthesized at various ion beam accelerating voltages and current densities. Figs. 2A and 2B show a set of data from these

analyses, identifying the synthesized nanowires with diameter smaller than 200 nm pure indium single crystals. Nanowires with larger diameters are polycrystalline. Moreover, electron energy loss spectroscopy (EELS) analysis was used to investigate the chemical compositions of the nanowires and the surface layer before and after FIB irradiation (Fig. 2C). Prior to FIB irradiation, the InGaN layers are saturated with ~80% indium content of (denoted by red color in Fig. 2C). After irradiation, essentially all the indium is diffused through the substrate pores producing pure indium nanowires. This can be explained as follows. Upon exposure to Ga^+ FIB, phase decomposition^[22, 23] occurs in the InGaN with the weaker bond between In and N broken readily producing indium. The indium easily diffuses through pores of surface layer, while GaN remains in the substrate. It is assumed that the nanowires must grow at the bottom of the wire where it is attached to the substrate fed by indium from the substrate. Exhaustion the indium in the InGaN layer is closely related to the length of the synthesized nanowires. The details of the mechanisms underpinning this phenomenon have not been explored.

In Figure 3, the geometrical characteristics and growth rate of synthesized nanowires have been plotted as a function of Ga^+ ion beam parameters, namely ion current density and accelerating voltage. Figure 3A shows the length of individual straight nanowires synthesized on a $420\ \mu\text{m} \times 360\ \mu\text{m}$ area by FIB irradiation with various accelerating voltages at a fixed ion current density of $15\text{nA}/\text{cm}^2$. At this ion current density, the average length of the synthesized nanowires increases by increasing the accelerating voltage: from $0.503\ \mu\text{m}$ at 5 kV to $60.28\ \mu\text{m}$ at 30 kV (The plot displays that length such that 10% of the wires have equal or larger length). Furthermore, straight nanowires with lengths greater than $100\ \mu\text{m}$ were synthesized for acceleration voltages of 20 kV and 30 kV. The density of indium nanowires synthesized at all four accelerating voltages was also estimated (Fig. 3A). At a low accelerating voltage of 5 kV, the nanowire density, defined as number of wires per unit area, is $\sim 5.76/\mu\text{m}^2$. While for all other three accelerating voltages, the nanowires density is at least

one order of magnitude lower and decreases by increasing the accelerating voltage. A simple calculation for the total mass of the synthesized nanowires per unit area based on the average diameter and length of the nanowires and the measured density yields $2.20 \times 10^{-2} \text{ g/m}^2$ and $8.68 \times 10^{-2} \text{ g/m}^2$ for the accelerating voltage of 5 and 30 kV, which are in the same order of magnitude as the indium content in the surface layer. We further measured the average length and diameter of the synthesized nanowires over a wider range of ion beam parameters. The results are summarized in Fig. 3B. The dimensions of the synthesized nanowires depend on the ion beam parameters in a complex fashion. For current density of 35 nA/cm^2 , increasing the accelerating voltage leads to thicker and longer indium nanowires, suggesting that the accelerating voltage is closely tied to the driving force in the process. This trend diminishes at higher current densities, since at high accelerating voltage and current density, the Ga^+ ions etch the indium nanowires as well as the InGaN surface. This effect becomes significant at voltages exceeding 20 kV for current densities 350 nA/cm^2 and higher. In this range the effect of cutting and etching becomes dominant undermining the growth rate which is driven by accelerating voltage.^[24, 25]

Finally, the average growth rate of the nanowires was measured over a range of ion beam parameters, Fig. 3C. Here, the growth rate is averaged over 5 distinct sets of experiment, all having the same ion current and accelerating voltage. The measured growth rate is an intricate function of ion beam parameters due to the complex interplay of the growth and erosion mechanisms discussed above. For example at the fixed voltage of 10 kV, the growth rate increases monotonically from 50 nm/s to 400 nm/s as the ion current density is increased from 15 to 7000 nA/cm^2 . Further increase in the current density leads to gradual reduction of the growth rate as the surface of InGaN substrate started to be milled(eroded) by FIB irradiation, leading to considerable morphological changes of the substrate surface. The maximum growth rate achieved in the range of ion beam parameters in Fig. 3C is $\sim 500 \text{ nm/s}$ at the accelerating voltage of 20 kV and current density of 2000 nA/cm^2 . This growth rate is

Submitted to
several orders faster than the current techniques.^[12, 26, 27] (See Fig. 1 and Supporting Information Movie S1)

As a final step, we controlled the growth region of individual indium nanowires using the method of maskless patterning built into the FIB system. When the InGaN surface is subject to the cross-shaped FIB irradiation shown in Fig. 4A, single nanowires emerge and grow at the center of the irradiated areas due to FIB overlapping.^[28] In this set of experiment, the ion beam was raster-scanned over the cross-shaped area from left to right and from top to bottom, leading to increased ion concentration at the center of the cross-shaped region. This method enables selection of the site of growth of individual nanowires. In Fig. 4A the current density and accelerating voltage are $1.2 \mu\text{A}/\text{cm}^2$ and 10 kV, which results in indium nanowires with average diameter and length of 80 nm and 6 μm , respectively. The average growth rate is 30 nm/s in this case. This method of creation of well-defined functional networks of nanowires has a significant potential in a number of scientific fields and technological applications, such as electronics and optoelectronic devices.^[5, 15-21] Site-controlled indium nanowires can be also used for assisting the growth of aligned long nanotubes due to their low melting point using Vapor-Liquid-Solid mechanisms.^[28-30] This method can be used for building nano-thermometer devices, opening new avenues for designing novel temperature-driven switches and sensors.^[17, 31] Furthermore using the maskless patterning method, we have created blocks of $25 \times 25 \mu\text{m}^2$ nanowire forests, Fig. 4B. In this case Ga^+ ion beam with accelerating voltage and current density of 5 KV and $350 \text{ nA}/\text{cm}^2$, respectively, was raster-scanned over areas of the substrate. The fabricated nanowires have average length and diameter of 2~3 microns and 50 nm, respectively.

In conclusion, we provide a method for controlled fabrication of straight indium nanowires on selected areas of the substrate. The growth rate of nanowires in this method is much higher than by currently available techniques. Extension of the developed technique allows for fabrication of variety of functional networks of indium nanowires, with control

over individual nanowires sites and dimensions. We briefly outlined potential implications of the developed technique, which can impact the current state of the art for building functional nanodevices.

Experimental

Preparation of InGaN layer: Indium rich InGaN layers of 300 nm thickness were grown epitaxially on a GaN/sapphire substrate with thickness 330 μm at 650 $^{\circ}\text{C}$ by metal-organic chemical vapor deposition (MOCVD). Trimethylgallium (TMGa), Trimethylindium (TMIn) and ammonia were used as Ga, In and N sources, respectively, and the input flow rates of TMGa, TMIn and NH_3 were 1.5 sccm, 225 sccm and 3 slm, respectively. Synthesized InGaN layers are saturated with ~80% indium confirmed by X-ray diffraction technique, and its roughness in RMS scale was measured as 30nm using Atomic Force Microscopy (AutoProbe CP research system, ThermoMicroscopes).

Focused ion beam irradiation: Indium rich InGaN layers were exposed to FIB of Ga^+ ion with various ion current densities and accelerating voltages at room temperature using high resolution FIB/FE-SEM dual beam system equipped with a Ga liquid metal source (Nova NanoLab 200, FEI). Pressure range inside the vacuum chamber was maintained within 2.0×10^{-4} to 6.0×10^{-4} Pa during the experiment. During exposure to FIB, the formation of nanowires was monitored *in-situ* by a FE-SEM system.

Characterization of synthesized nanowires: For performing TEM analysis, the target single nanowire was isolated from the InGaN layer by a manipulating probe (Model 100.7TM, Omniprobe). The thickness of nanowires was reduced to 5~60 nm by milling using FIB for the analysis in TEM and EDS. This procedure was performed at the temperature of -90 $^{\circ}\text{C}$, using a cooling stage to prevent the nanowire from melting with high temperature during milling. Then, the cross-section of the nanowires with the thickness ~60 nm was examined

using TEM (JEM-3000F, JEOL). The chemical composition of nanowires was analyzed using energy dispersive x-ray spectroscopy (EDS, OXFORD). The structural properties of nanowires were confirmed by high-resolution TEM and electron diffraction pattern. The compositional change of InGaN layer during FIB irradiation was examined by electron energy loss spectroscopy (EELS) using high voltage electron microscope (HVEM, JEOL).

Creation of functional networks of nanowires: Functional network of individual nanowires were created by adopting the maskless patterning method of the FIB equipment. This method permits the accurate selection of the areas exposed to FIB. The bitmap file of the exposure pattern was imported as a virtual mask in the FIB system. The ion beam was raster-scanned over the cross-shaped area with dwell time of 1 μ s.

Received: ((will be filled in by the editorial staff))

Revised: ((will be filled in by the editorial staff))

Published online: ((will be filled in by the editorial staff))

- [1] C. M. Lieber, *MRS Bull.* **2003**, 28, 486.
- [2] Y. Xia, P. Yang, Y. Sun, Y. Wu, B. Mayers, B. Gates, Y. Yin, F. Kim, H. Yan, *Adv. Mater.* **2003**, 15, 353.
- [3] H. J. Fan, P. Werner, M. Zacharias, *Small* **2006**, 2, 700.
- [4] F. Patolsky, B. P. Timko, G. Zheng, C. M. Lieber, *MRS Bull.* **2007**, 32, 142.
- [5] A. Javey, S. Nam, R. S. Friedman, H. Yan, C. M. Lieber, *Nano Lett.* **2007**, 7, 773.
- [6] A. K. Geim, I. V. Grigorieva, S. V. Dubonos, J. G. S. Lok, J. C. Maan, A. E. Filippov, F. M. Peeters, *Nature* **1997**, 390, 259.
- [7] A. P. Alivisatos, P. F. Barbara, A. W. Castleman, J. Chang, D. A. Dixon, M. L. Klein, G. L. McLendon, J. S. Miller, M. A. Ratner, P. J. Rossky, S. I. Stupp, M. E. Thompson, *Adv. Mater.* **1998**, 10, 1297.
- [8] J. Hu, T. W. Odom, C. M. Lieber, *Acc. Chem. Res.* **1999**, 32, 435.

- [9] R. Agarwal, C. M. Lieber, *Appl. Phys. A* **2006**, 85, 209.
- [10] I. Obataya, C. Nakamura, S. Han, N. Nakamura, J. Miyake, *Nano Lett.* **2005**, 5, 27.
- [11] G. Zheng, F. Patolsky, Y. Cui, W. U. Wang, C. M. Lieber, *Nat. Biotechnol.* **2005**, 23, 1294.
- [12] G. Yi, W. Schwarzacher, *Appl. Phys. Lett.* **1999**, 74, 1746.
- [13] N. Giordano, *Phys. Rev. Lett.* **1988**, 61, 2137.
- [14] M. Tinkham, in *Introduction to superconductivity 2nd Edition*, McGraw-Hill, New York, **1996**.
- [15] S. Vaddiraju, A. Mohite, A. Chin, M. Meyyappan, G. Sumanasekera, B. W. Alphenaar, M. K. Sunkara, *Nano. Lett.* **2005**, 5, 1625.
- [16] G. Cheng, E. Stern, D. Turner-Evans, M. A. Reed, *Appl. Phys. Lett.* **2005**, 87, 253103.
- [17] Y. Li, Y. Bando, D. Golberg, *Adv. Mater.* **2003**, 15, 581.
- [18] D. Zhang, Z. Liu, C. Li, T. Tang, X. Liu, S. Han, B. Lei, C. Zhou, *Nano. Lett.* **2004**, 4, 1919.
- [19] P. Nguyen, H. T. Ng, T. Yamada, M. K. Smith, J. Li, J. Han, M. Meyyappan, *Nano. Lett.* **2004**, 4, 651.
- [20] J. Wang, M. S. Gudiksen, X. Duan, Y. Cui, C. M. Lieber, *Science* **2001**, 293, 1455.
- [21] H. Pettersson, J. Trägårdh, A. I. Persson, L. Landin, D. Hessman, L. Samuelson, *Nano. Lett.* **2006**, 6, 229.
- [22] J. Lian, W. Zhou, Q. M. Wei, L. M. Wang, L. A. Boatner, R. C. Ewing, *Appl. Phys. Lett.* **2006**, 88, 093112.
- [23] A. Lugstein, B. Basnar, E. Bertagnolli, *Nucl. Instrum. Methods Phys. Res. Sect. B-Beam Interact. Mater. Atoms* **2004**, 217, 402.
- [24] A. A. Tseng, *Small* **2005**, 10, 924.
- [25] L. Frey, C. Lehrer, H. Ryssel., *Appl. Phys. A-Mater. Sci. Process.* **2003**, 76, 1017.
- [26] C. Y. Nam, J. Y. Kim, J. E. Fischer, *Appl. Phys. Lett.* **2005**, 86, 193112.

- [27] K. Soulantica, A. Maisonnat, F. Senocq, M. –C. Fromen, M. –J. Casanove, B. Chaudret, *Angew. Chem. Int. Ed.* **2001**, *40*, 2984.
- [28] R. Buckmaster, T. Hanada, Y. Kawazoe, M. Cho, T. Yao, N. Urushihara, A. Yamamoto, *Nano. Lett.* **2005**, *5*, 771.
- [29] S. D. Dingman, N. P. Rath, P. D. Markowitz, P. C. Gibbons, W. E. Buhro, *Angew. Chem. Int. Ed.* **2000**, *39*, 1470.
- [30] Y. Li, Y. Bando, D. Golberg, *Adv. Mater.* **2004**, *16*, 37.
- [31] J. Zhan, Y. Bando, J. Hu, Z. Liu, L. Yin, D. Golberg, *Angew. Chem. Int. Ed.* **2005**, *44*, 2140.

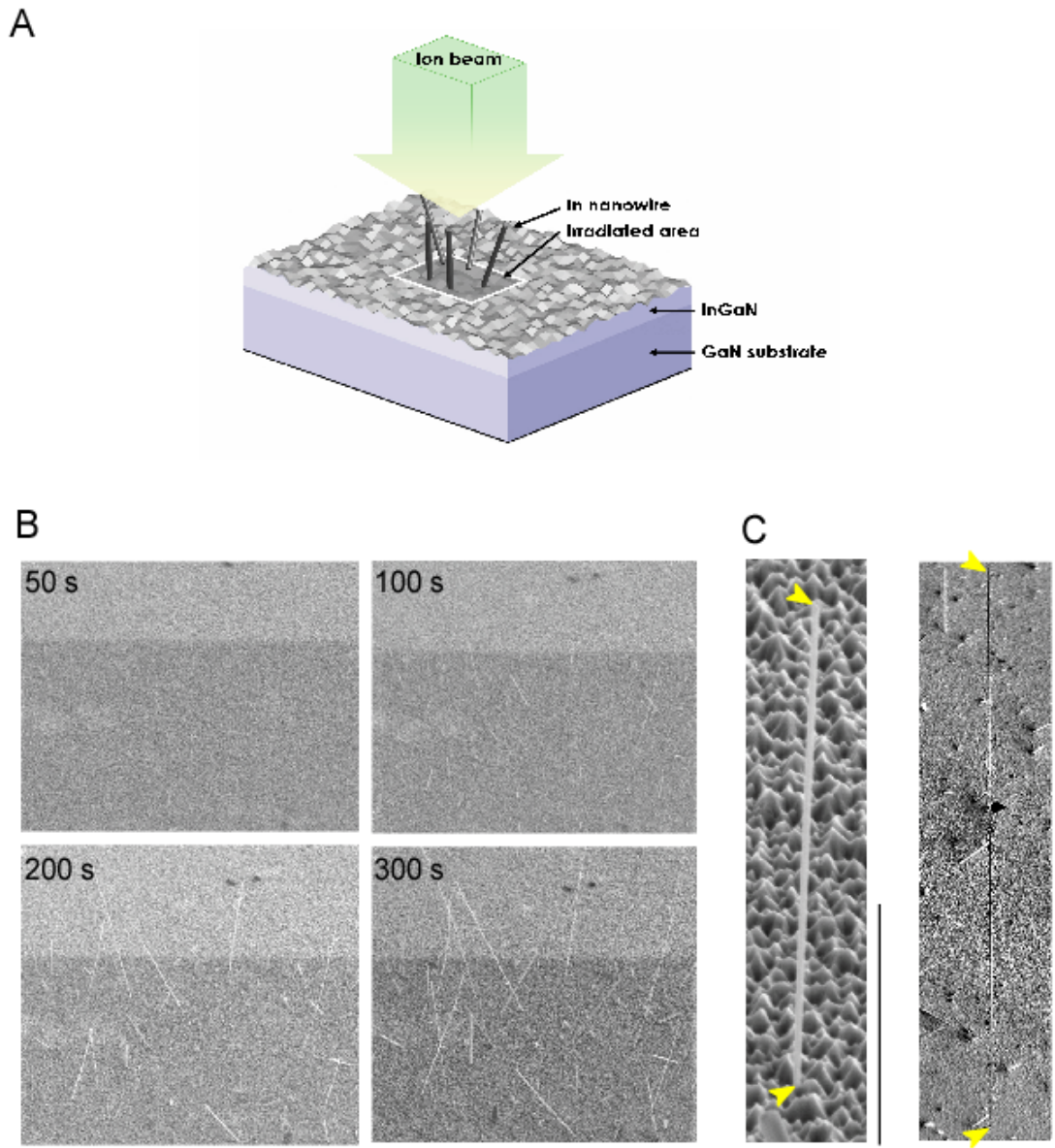


Figure 1. Fabrication of indium nanowires by focused ion beam irradiation. (A)

Schematic of the experiment. Straight nanowires appear on the surface area of the InGaN

layer exposed to FIB. (B) Time evolution of formation of straight nanowires after exposure to

FIB with accelerating voltage of 10 kV and ion current density of 200 nA/cm^2 . The area

subject to FIB is $42 \mu\text{m} \times 36 \mu\text{m}$. Scale bar=20 microns. (C) Single Nanowires with length and

diameter of $20 \mu\text{m}$ and 100 nm (left) and $130 \mu\text{m}$ and 300 nm (right) created by focused ion

beam irradiation. Arrow heads show the top and bottom of the nanowires. Scale bar=10

microns.

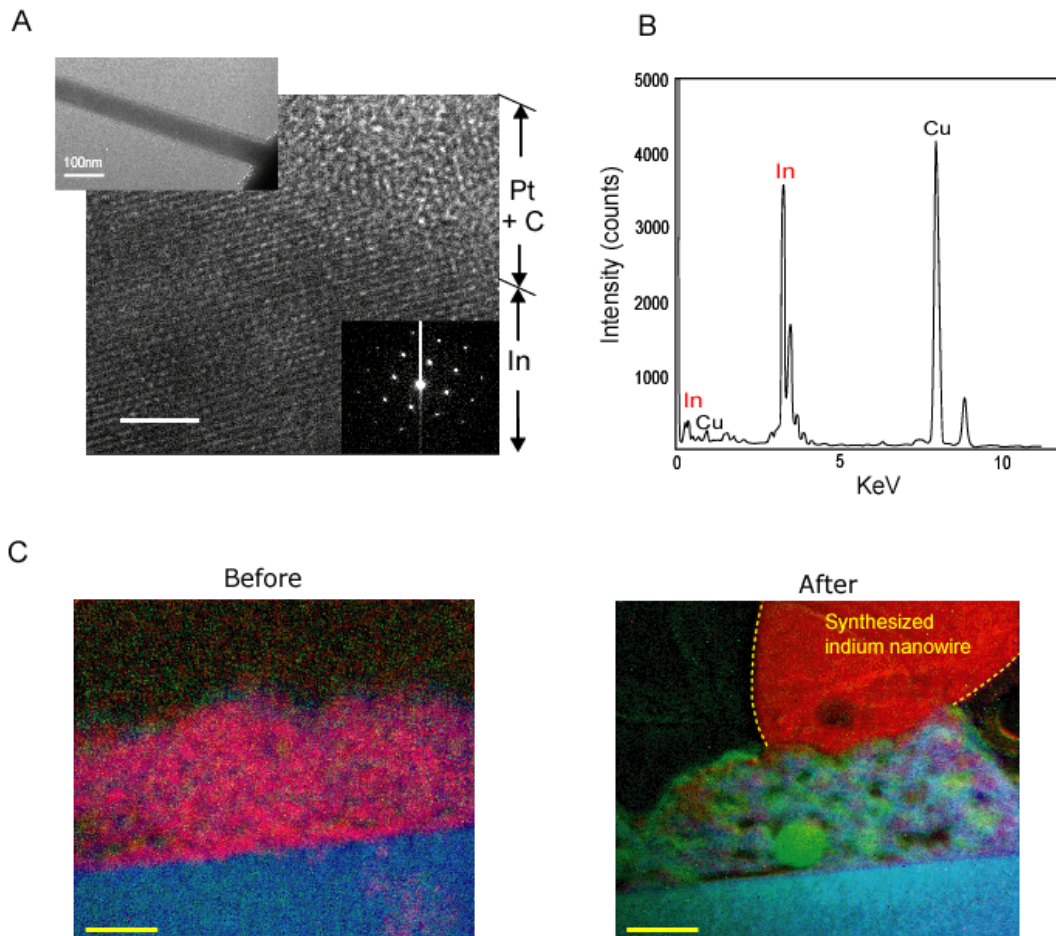


Figure 2. Characterization of synthesized nanowires. (A) TEM analysis of the nanowire cross section. Electron diffraction pattern of a nanowire with [110] zone axis confirms that the single crystal grows in the $[-1\ 1\ 2]$ direction. The crystal has body-centered tetragonal structure with lattice constants measured as $a = 0.325$ nm and $c = 0.495$ nm, matching the reported values for bulk indium crystals (JCPDS No.5-642). Scale bar= 2 nm. (B) EDS spectrum detected in the central region of a cross-sectioned nanowire. The results verify that the wire is pure indium. The presence of copper is believed to derive from the Cu TEM grid. (C) EELS analysis of InGaN substrate before and after focused ion beam irradiation. The color labels of red, green and blue denote indium (In), gallium (Ga) and nitrogen (N), respectively. Prior to ion beam irradiation, over 80 % of the InGaN layer is indium (red). After 15 minutes irradiation of Ga⁺ FIB, Gallium (green) and Nitrogen (blue) were detected below the surface inside the layer, while the indium exists only in the body of the nanowire (red). Scale bar= 100 nm.

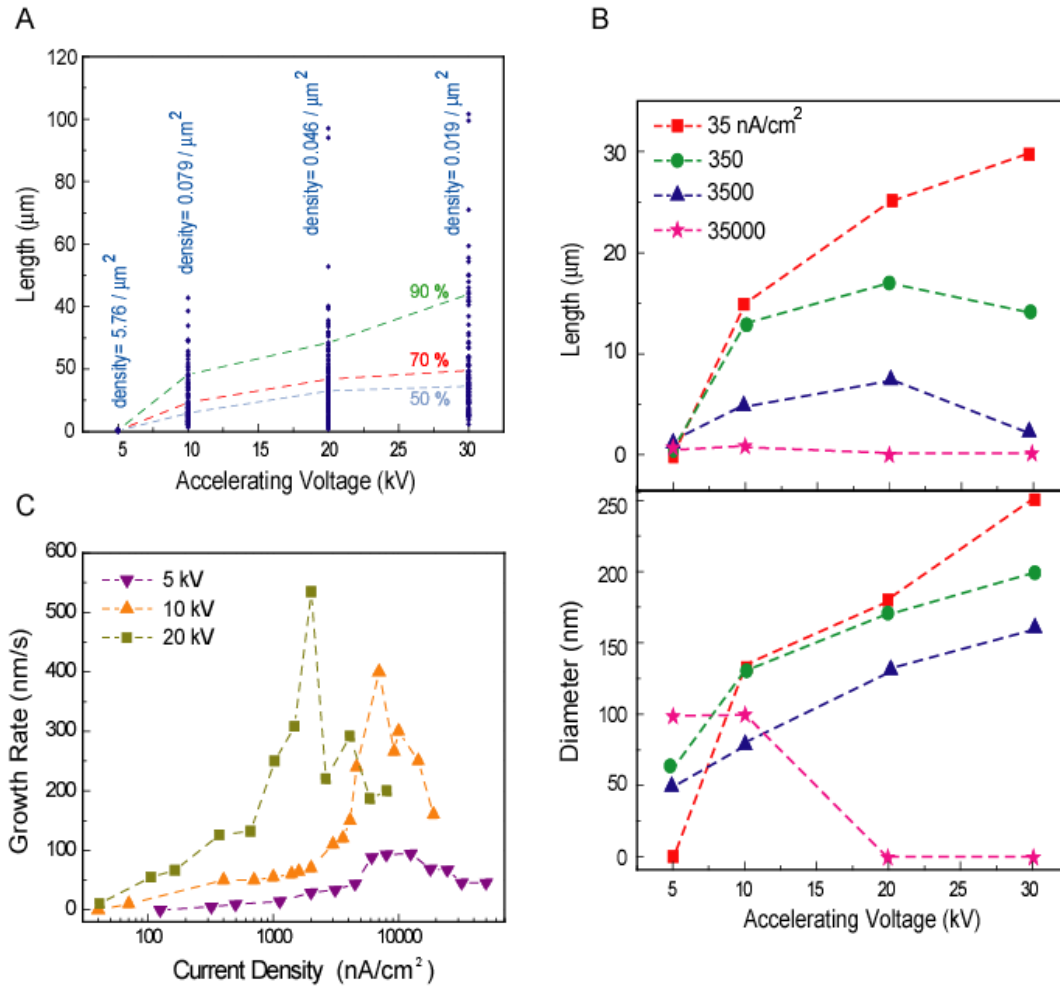


Figure 3. Dependence of the nanowires dimensions and growth rate on the ion beam parameters. (A) Length distribution of the nanowires synthesized at current density of 15 nA/cm² and different ion beam accelerating voltages. 50% line corresponds to the median of the nanowires length at each accelerating voltage. The lines denoted by 70% and 90% indicate the 70th and 90th percentile of the collected data for nanowires length at each accelerating voltage. The density of the nanowires defined as the number of nanowires/unit area is estimated for each case. (B) Dependence of nanowires average length and diameter on the ion beam parameters. The reported length is the 90th percentile of the collected data. (C) Dependence of the average growth rate of nanowires on the ion beam current density measured for three distinct voltages of 5, 10, 20 kV. Here, the average growth rate for each nanowire is estimated as the total length divided by total growth time.

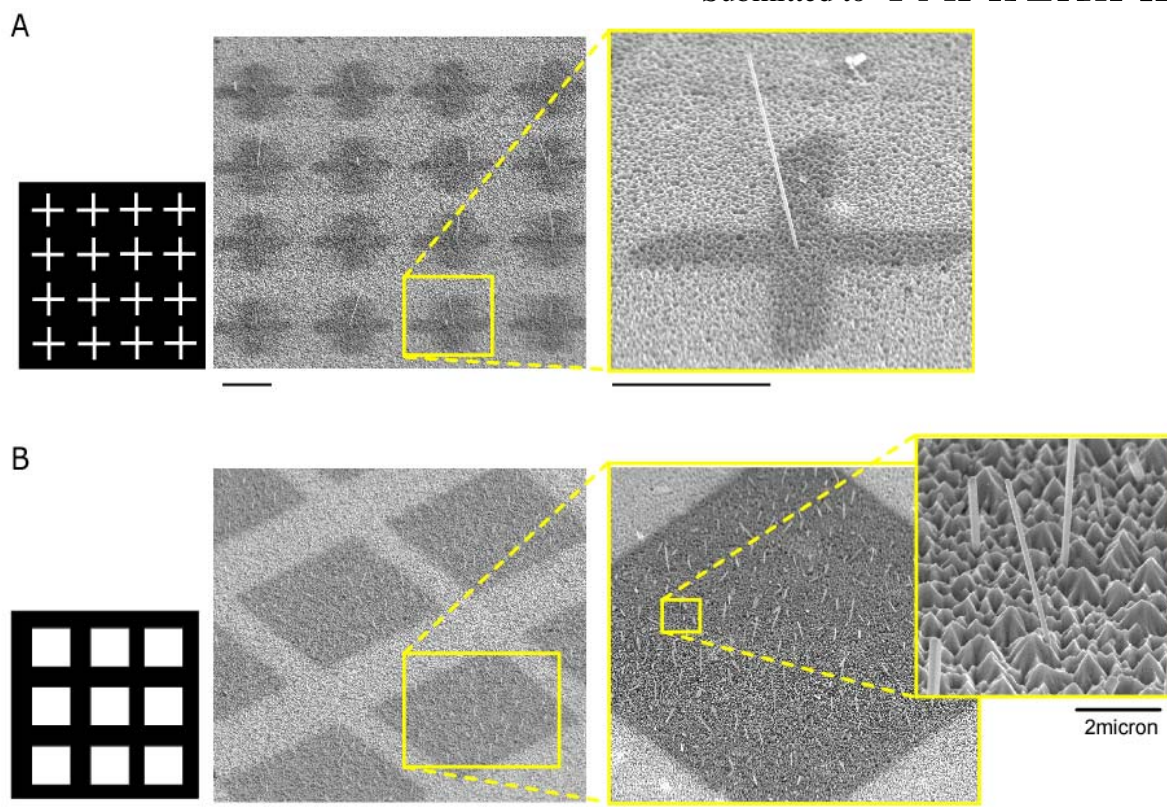


Figure 4. Functional networks of nanowires. (A) Scanning Electron Microscopy image of a network of single indium nanowires created on selected locations of the InGaN layer using maskless patterning method. A bitmap with crossed bars of 500 nm width and 12.5 μm length with the desired pattern (shown on left) were imported to the FIB such that only the white regions were exposed to the ion beam. (B) Nanowire forests of 25 x 25 μm size. The synthesized nanowires have an average length and diameter of 2~3 microns and 50 nm, respectively (right of (B)). In both experiments, The current density and accelerating voltage of ion beam are 1.2 $\mu\text{A}/\text{cm}^2$ and 10 kV for (A) and 350 nA/cm^2 and 5 KV for (B). (See **SMovie 2**). Bar=5 micron if not denoted otherwise.

Supporting Information

Movie S1.

Growth of indium nanowires on the surface by exposure to ion beam. The ion beam has the accelerating voltage of 10 kV and current density of 400 nA/cm^2 . The average growth rate is

50 nm/s and the total irradiation time is 260s, with first appearance of nanowires occurring at 80 seconds.

Movie S2.

Single indium nanowires synthesized at the junctions of the grid pattern using focused ion beam irradiation. The ion beam has the accelerating voltage of 10 kV and current density of $1.2 \mu\text{A}/\text{cm}^2$. The frames were acquired at interval of 7s.